Yu, R., Grytsai, A., Milinevsky, G., Evtushevsky, O., Yukhymchuk, Yu., Zazubyk, D., & Klekociuk, A. (2025). Comparison of Antarctic total ozone behavior in pre-SSW, SSW, and post-SSW years.
*Ukrainian Antarctic Journal*, *23*(2), 30–52.
https://doi.org/10.33275/1727-7485.2.2025.749





# Comparison of Antarctic total ozone behavior in pre-SSW, SSW, and post-SSW years

**Ruixian Yu**[1], **Asen Grytsai**[2, 3], **Gennadi Milinevsky**[1, 2, 4, *], **Oleksandr Evtushevsky**[3], **Yuliia Yukhymchuk**[1, 4, **], **Diana Zazubyk**[3], **Andrew Klekociuk**[5]

[1] College of Physics, International Center of Future Science, Jilin University, Changchun, 130012, China
[2] State Institution National Antarctic Scientific Center, Ministry of Education and Science of Ukraine, Kyiv, 01601, Ukraine
[3] Taras Shevchenko National University of Kyiv, Kyiv, 01601, Ukraine
[4] Main Astronomical Observatory of National Academy of Sciences of Ukraine, Kyiv, 03143, Ukraine
[5] School of Physics, Chemistry and Earth Science, The University of Adelaide, Adelaide, 5005, Australia

**Corresponding authors:** * milinevskyi@jlu.edu.cn, genmilinevsky@gmail.com; ** yukhymchuk@jlu.edu.cn

**Abstract.** Sudden stratospheric warmings (SSWs) are dramatic events characterized by sudden and sharp changes in the distribution of polar stratospheric temperatures, zonal winds, total ozone column, and other atmospheric parameters. SSWs are usual in the winter season in the Northern Hemisphere, but they are rare in the Antarctic stratosphere. Only one major SSW (September 2002) was observed in the southern polar stratosphere over the entire time of observations. In the paper, this event is considered in conjunction with the warmings of 1988 and 2019, which do not correspond to the major SSW definition, but were accompanied by significant temperature and total ozone increases, as well as zonal wind deceleration. The changes in the total ozone distributions over Antarctica are analyzed using Multi-Sensor Reanalysis (MSR-2) data. We have plotted and analyzed the spatial distribution of total ozone anomalies in the SSW years and adjacent years. A significant zonal asymmetry is noted between the Western and Eastern Hemispheres over Antarctica. In the East Antarctic stratosphere, total ozone increases several weeks before the central date of the warming, indicating preconditions for the event. Quasi-periodic oscillations associated with planetary waves were observed over East Antarctica in 1988 and 2002. On the contrary, total ozone over West Antarctica showed no clear features prior to the warming. The warmings have distinct spatial coverage: in particular, the 1988 event did not penetrate the inner region of the stratospheric polar vortex. In the adjacent years, total ozone was predominantly lower than climatological values, and we have concluded that total ozone decrease is most typical for the previous years (1987, 2001, 2018).

**Keywords:** Antarctic research stations, life cycle, MSR-2 overpass data, planetary waves, sudden stratospheric warming, total ozone column

## 1 Introduction

Sudden stratospheric warmings (SSWs) are large-scale disturbances of the polar stratosphere during winter months that occur approximately every second year in the Northern Hemisphere (NH) (Butler et al., 2017). This phenomenon is much less frequent in the Southern Hemisphere (SH)

(Jucker et al., 2021). There are various approaches to defining SSWs, based on criteria such as the reversal of the zonal-mean zonal wind, changes in the meridional temperature gradient, vertical profiles of temperature, geopotential height anomalies, and vortex parameters (Butler et al., 2015).

The World Meteorological Organization (WMO) gave the primary definition of an SSW event. It requires a stratosphere temperature increase and zonal wind reversal to easterlies at the 10-hPa pressure level (~30 km altitude) and 60° latitude (WMO, 1978). This definition was discussed and detailed in several papers (Butler et al., 2015; 2017; Butler & Gerber, 2018). One of the frequently used definitions (Charlton & Polvani, 2007) identifies a major SSW as an event when the zonal-mean zonal wind at 60° latitude at the 10-hPa pressure level reverses to easterly during November–March (in the NH) and subsequently returns to westerly before 20 April. The Charlton and Polvani (2007) criterion does not require a reversal of the temperature gradient, and two different SSW events must be separated by at least 20 days.

The first observed SSW in the SH occurred in 1988. This SSW cannot be classified as a major event because no reversal of the zonal mean wind to easterly was observed. However, a significant stratosphere temperature rises by 59 °C in 10 days, and a total ozone column (TOC) increase by 227 Dobson units (DU) in 9 days, which is even higher than in the NH, were observed at the Antarctic Syowa Station (Kanzawa & Kawaguchi, 1990). The TOC monthly mean value increased significantly compared to the previous year and was close to the values of the 1970s. The authors found a good correlation between total ozone and temperature oscillations, which may indicate that such changes occur because of planetary wave dynamical transport effects.

From the middle of the 1988 austral winter, Total Ozone Mapping Spectrometer (TOMS) satellite data demonstrated the formation of a warm stationary ridge in the lower stratosphere in the region to the south of Australia. Satellite aerosol measurements showed a low amount of polar stratospheric clouds (PSCs) inside the polar vortex. Increased stratospheric temperatures, mid-latitude air transport, and a reduction in the probability of PSC formation led to a significant reduction of the ozone hole size (Schoeberl, 1988).

Only one event in the SH can be classified as a major SSW. In September 2002, the zonal-mean zonal wind had reversed from westerly to weak easterly and had been very disturbed a few months prior. During this event, the temperatures near the edge of the polar vortex were considerably higher than usual, and the polar night jet was weak, leading to the smallest ozone hole observed since 1988 (Newman & Nash, 2005). Both the ozone hole and the polar vortex split into two parts. A few smaller warming events occurred from late August to mid-September in 2002, with a similar amplitude to events in 1988 before the major SSW (Baldwin et al., 2003).

Another outstanding SSW event occurred in September 2019. The zonal-mean zonal wind did not reverse to easterly, so it may only be considered as minor (Shen et al., 2020a). However, the decrease in ozone hole area was higher than in either 2002 or 1988 SSW. The increase in the 10-hPa temperature during mid-to-late September was comparable to those of previous SSWs in the SH, but the difference from the climatology was noticeably higher. This event is considered to be the strongest polar cap warming observed in the Southern Hemisphere (Shen et al., 2020b; Ma et al., 2022; Yu et al., 2025). During the 2019 SSW, a weakening of the polar vortex in the Southern Hemisphere led to a slowing of the jet stream and a sharp warming in the middle stratosphere, triggered by planetary wave 1. These events impacted the troposphere, providing extreme warming in Australia (Lim et al., 2021).

Due to the ozone hole still appearing over Antarctica since the mid-1980s, it is essential to study TOC temporal and spatial characteristics in the region to understand regional and global atmospheric changes and to compare the years before the SSW events (pre-SSW years), SSW years (1988, 2002, 2019), and post-SSW years. This study ex-

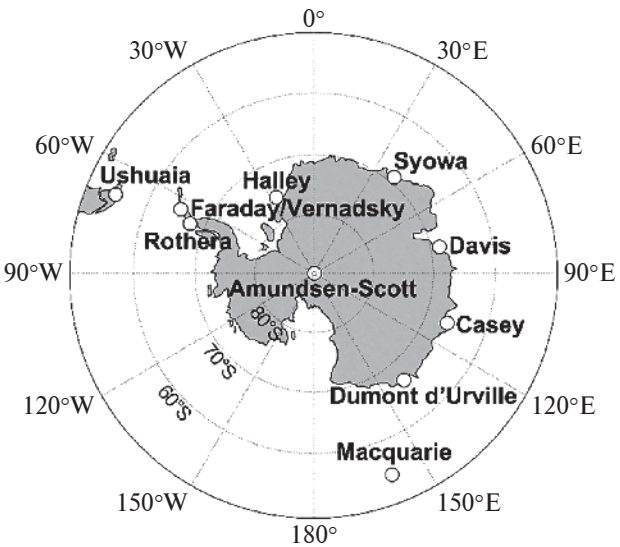


**Figure 1.** Stations measuring TOC chosen for the study

plores the association between SSW events and TOC variations over Antarctica at ten stations (Fig. 1).

The variations of the September average ozone values for these ten stations for each SSW year and non-SSW years are shown in Figure 2a. In SSW years, the ozone values are significantly higher than in non-SSW years. Also, the September zonal-mean zonal wind are lowest in SSW years (Fig. 2b). However, TOC variations significantly depend on a station's geographical location. The trend and variations in TOC may lead to or serve as a precursor to an SSW occurrence. Because SSW events strongly impact atmospheric conditions, including dynamics, chemistry, and composition, SSW frequency in both polar regions and the possibility of discovering a 'precursor' for SSW events are still critical problems for study.

This paper aims to look for (1) signs (precursors) of SSW emergence based on data for the pre-SSW years, and (2) evidence of SSW post-effects. That is, could the atmosphere over Antarctica in the year of the SSW "remember" what happened to the ozone hole and ozone content in the previous year, and could it "feel" the SSW consequences in the following year? So, a key question is whether there is a particular difference between the pre-SSW, SSW, and post-SSW years. We also expand results of the paper of Yu et al. (2025), considering in more detail spatial distribution of total ozone anomalies near the dates of SSW. Ozone depletion tends to peak around late September (see, for example, https://www.temis.nl/protocols/o3hole/), which is possibly a reason behind some consistency in the behavior of the non-SSW years relative to the onset (zero-lag) date.

The data and methods used in this study are described in Section 2. In Section 3, we present results considering the planetary wave activity and analyzing the TOC values at ten stations in pre-SSW, SSW, and post-SSW years. Section 4 discusses the results, explaining variations of TOC, followed by conclusions.

## 2 Data and methods

We use Multi-Sensor Reanalysis (MSR-2) data to study total ozone variations in Antarctica in September–October. The data are taken for the location of eight Antarctic stations (Amundsen-Scott, Rothera, Faraday/Vernadsky, Halley, Syowa, Davis, Casey, and Dumont d'Urville) and two sub-Antarctic stations (Ushuaia and Macquarie Island), considering overpass data presented at the TEMIS service, MSR-2 (https://temis.nl/protocols/O3global.php). Averaging TOC values by calculating arithmetic means from the overpasses for all the Antarctic stations is used. In addition, TOC means in similar way are obtained separately for West Antarctica (Amundsen-Scott, Rothera, Faraday/Vernadsky, Halley, Ushuaia) and East Antarctica (Syowa, Davis, Casey, Dumont d'Urville, and Macquarie Island). To characterize regional TOC variability more completely, we also use the MSR-2 total ozone field south of the 50°S latitude. The ozone values for the study range from 1979 to 2022 in September, when three prominent SSW events occurred in 1988, 2002, and 2019. These stations are permanently occupied, and a motivation for choosing them is that the influence of SSW events on TOC is relevant to the health effects of ultraviolet radiation. To study TOC changes be-

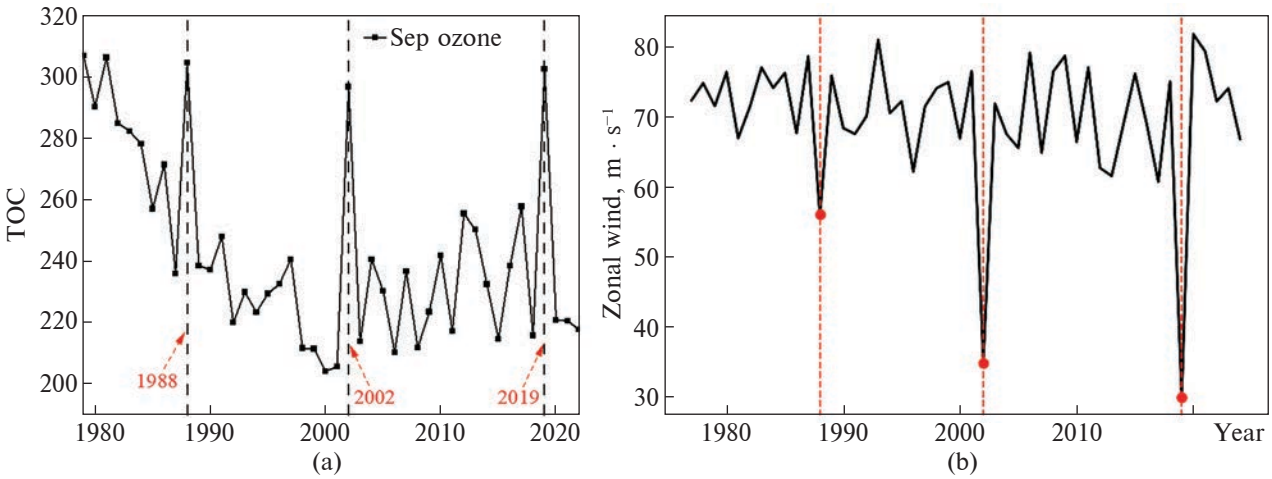


**Figure 2.** September average (a) total ozone column (TOC) values in DU for ten stations for SSW years (red marks) and non-SSW years, (b) zonal wind at 60°S latitude by ERA5 reanalysis has minimal values in SSW years 1988, 2002, and 2019 (red dots)

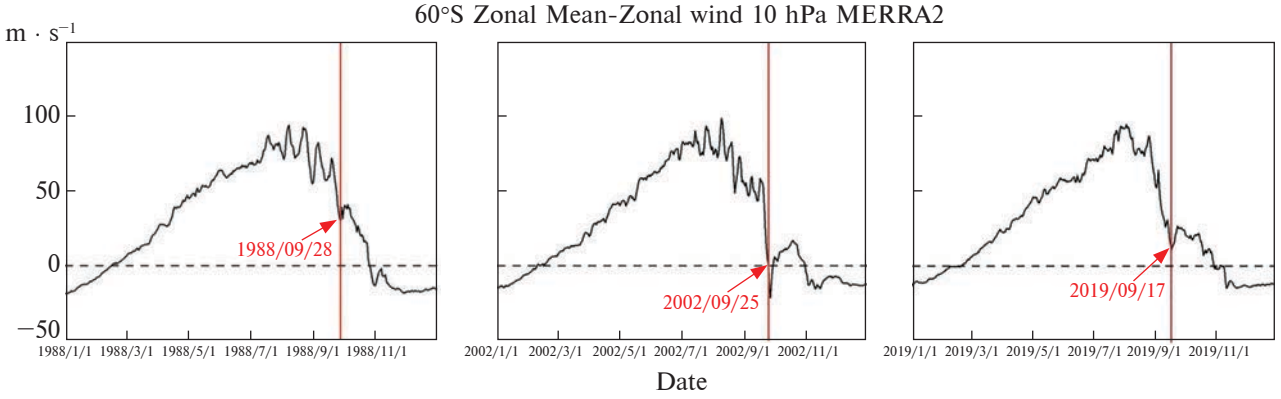


**Figure 3.** Zonal wind at 10 hPa for the three largest stratospheric warming events by the MERRA2 data. Red vertical lines mark the dates of wind slowing down or reversing

fore and after an SSW event, we analyze the values during 60 days before and 60 days after the warming. We did not choose larger time intervals because late November typically corresponds to a clear weakening of the stratospheric polar vortex with the following total ozone distribution that is nearly uniform and similar for different years. The years of the noticeable warmings (1988, 2002, 2019) and adjacent to them (1987, 1989, 2001, 2003, 2018, 2020) were analyzed.

The onset dates of the SSW events were taken from Shen et al. (2020b), where the maximum temperatures during the early stage of the SSW events were determined on 28 September 1988, 29 September 2002, and 19 September 2019. It is important that the MERRA-2 temperature in the polar cap (60–90°S) at 10 hPa shows a local maximum on these days, and the westerly zonal wind at 60°S, 10 hPa has its local minimum on 28 September 1988, 29 September 2002, and 17 September 2019 (https://ozonewatch.gsfc.nasa.gov/meteorology/SH.html). Therefore, no significant time difference in dependence on choice of other SSW indicator, and these dates were chosen as onset (zero) dates in the figures for the adjacent non-SSW years, as well (similar to the consider-

ation in the paper by Yu et al., 2025). The date of zonal wind reversal in case of the 2002 SSW at 10 hPa is also considered (Fig. 3). Data from the MERRA2 reanalysis on zonal-mean zonal wind (Fig. 3) and planetary wave activity (obtained from geopotential height variations) discussed in the text were provided by the Atmospheric Chemistry and Dynamics Laboratory (https://acd-ext.gsfc.nasa.gov/), and they are discussed in the text. Mean values and quantiles (10%, 30%, 70%, 90%) are presented in this data (see Figs. A3.1, A3.2). El Niño – Southern Oscillation (ENSO; https://hadleyserver.metoffice.gov.uk/hadisst/); and quasi-biennial oscillation (QBO; cpc.ncep.noaa.gov/data/indices/qbo.u30.index) indices were considered. Importance of the phenomena is conditioned by their influence on the state of the stratospheric polar vortex.

To investigate the TOC field behavior over Antarctica during SSW events, we map MSR-2 data for total ozone anomalies for the ±15 days before and after the zero dates of SSWs against the 1979–2022 daily-averaged TOC climatology obtained for every point of the MSR-2 grid (spatial resolution is 0.5° in latitude and 0.5° in longitude) in the southern polar area south of 50°S. In these calculations of climatology, the three SSW years (1988, 2002, and 2019) were excluded. Further, we subtracted the climatology from the values for the corresponding day of the year in order to obtain total ozone anomalies. Let $i$ be day of year and $j$ be number of year (without the three years of SSW). Then, the climatological mean is determined as

$$\overline{X_i} = \sum_{j=1}^{n} X_{ij} / n.$$

In the following, ozone anomaly for a day $i$ in a year $k$ is calculated as $\delta X_{ik} = X_{ik} - \overline{X_i}$.

The resulting values (absolute difference in DU between TOC values and climatology) were mapped for the days −15, −10, −5, 0, +5, +10, +15 relative to the respective SSW zero date. For the pre-SSW and post-SSW years, the calculations were performed for the exact dates as in the adjacent year of the SSW event (for example, 29 September was considered as the zero date in 2001, 2002, and 2003). All maps are constructed using the same color scale to facilitate their comparison.

## 3 Results

### 3.1 TOC averaged at ten Antarctic stations over the SSW, pre-SSW, and post-SSW years

The upper panels of Figure 4 show the plots of TOC values averaged over all ten stations for each day within ±60 days relative to the SSW onset for the SSW year and the years before and after, respectively. The SSW onset date is the exact day when a major/minor SSW event begins, marked by a strong stratospheric warming and a reversal or significant slowdown of the winter polar vortex. In our plots and in the text, for the SSW onset date we also use the term “zero date” (“0” date on plots). In Figure 4, the green dotted lines are the climatological averages of the TOC from the ten stations during the period 1979–2022, excluding data from 1988, 2002, and 2019, for each day within ±60 days relative to the SSW onset.

The middle panel of Figure 4 plots TOC values averaged from five WH stations for each day within ±60 days relative to the SSW onset for the SSW year and the years before and after, respectively. The bottom panel of Figure 4 is similar to the middle panel, but for TOC values from five EH stations. TOC over Antarctica increased significantly during SSW years compared to the preceding and the following years.

The grey shaded area in Figure 4 indicates the TOC range between the 70th and 30th percentiles over the climatology. As shown in the grey-shaded area of Figure 4, the TOC ranges for the three SSW years exceed the 70th percentile over the climatology, indicating significantly larger TOC values during these SSW events. Conversely, the TOC ranges for the years adjacent to the SSW events are between the 70th and 30th percentiles or lower 30th percentile. The primary cause of TOC variations is attributed to ozone changes in the Eastern Hemisphere over Antarctica.

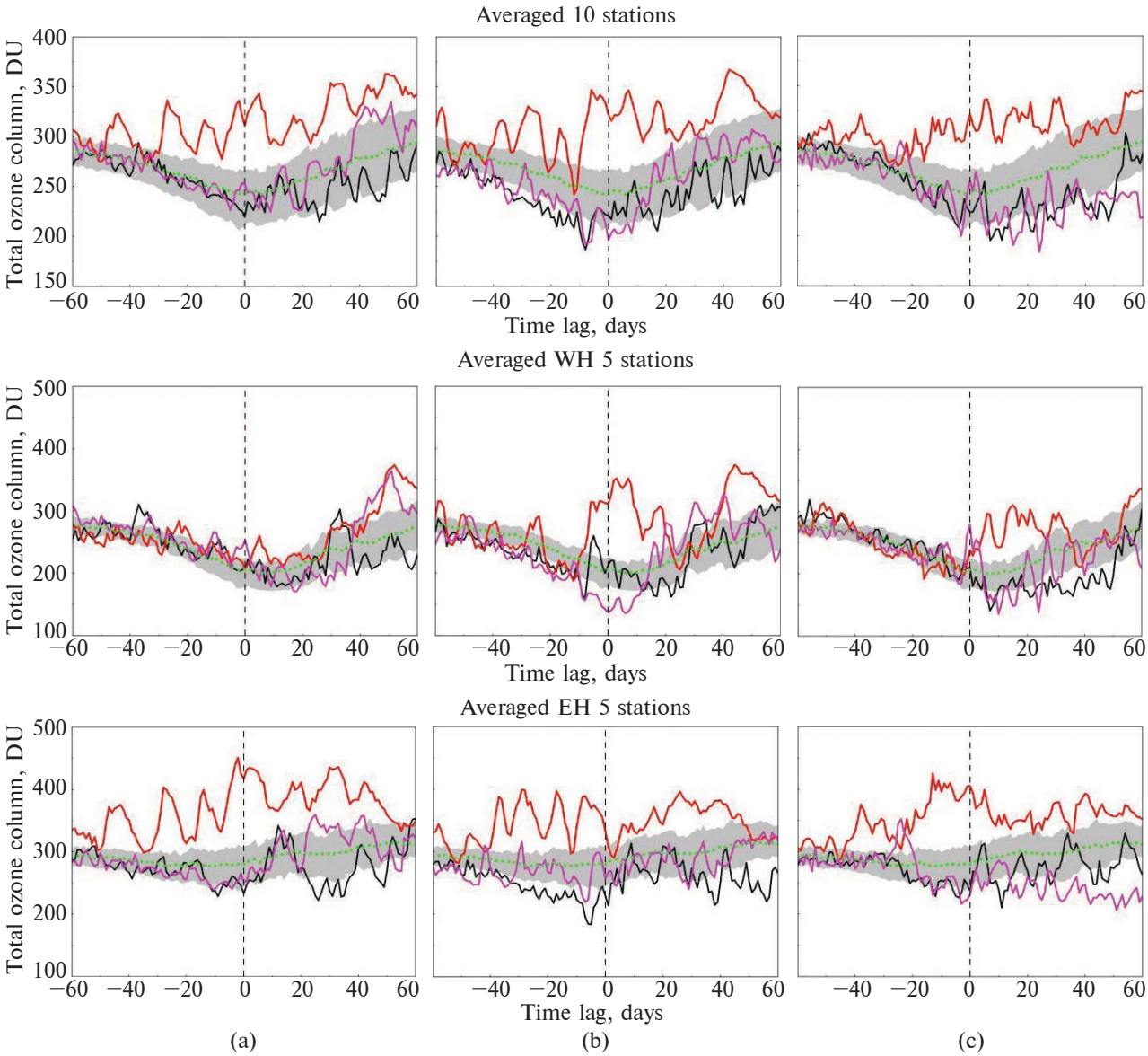


**Figure 4.** TOC values averaged over Antarctic ten stations (upper panel) and five stations in the Western Hemisphere (WH, middle panel) and Eastern Hemisphere (EH, bottom panel) for each day within ±60 days relative to the SSW onset for the SSW year and the years before and after SSW. The grey shaded area indicates the TOC range between the 70th and 30th percentiles over the climatology (green dotted line). Column (a) black line – 1987, red line – 1988 SSW, pink line – 1989; column (b) black line – 2001, red line – 2002 SSW, pink line – 2003; column (c) black line – 2018, red line – 2019 SSW, pink line – 2020

The SSW events of 1988 and 2019 were accompanied by exceptionally high planetary wave amplitudes at 50 hPa in September, with a prominent planetary wave 1 (see Figure A3.1 in Appendix 3). From Figure A3.2 in Appendix 3, the 2002 SSW event was associated with particularly strong activity of planetary wave 2. Moreover, the amplitudes of planetary wave during these SSW events were greater than those of the adjacent years, implying a potential correlation between the

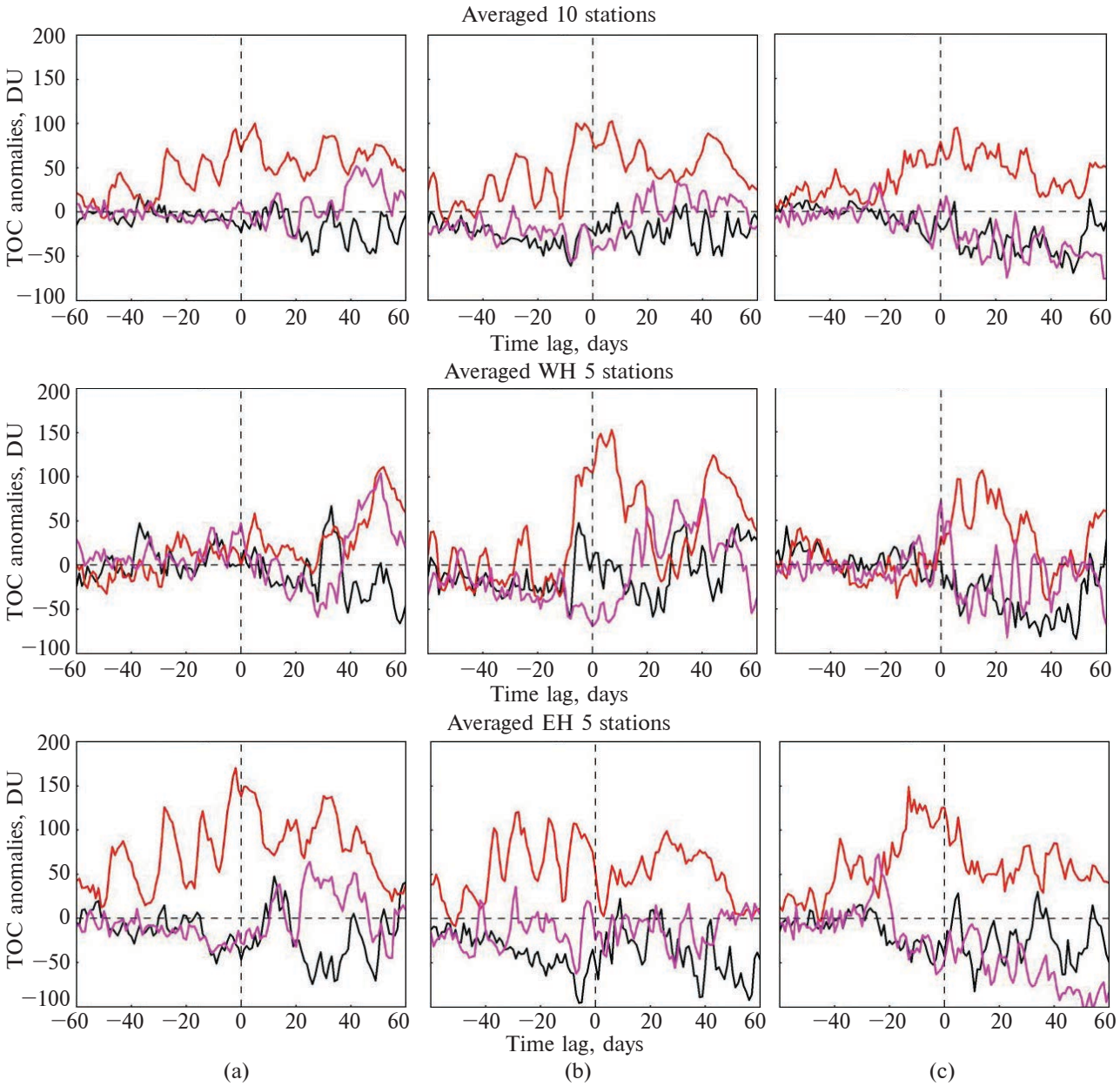


**Figure 5.** TOC anomaly values against 1979–2022 climatology averaged over ten Antarctic stations and five WH and EH stations for the SSW years and the years before and after SSW. Column (a) black line – 1987, red line – 1988 SSW, pink line – 1989; column (b) black line – 2001, red line – 2002 SSW, pink line – 2003; column (c) black line – 2018, red line – 2019 SSW, pink line – 2020

intensity of planetary wave activity and the magnitude of TOC increases.

As can be seen in the panels of Figure 4 by comparison with the climatological range between the 30th and 70th percentiles, the SSW years show anomalous episodic increases in ozone levels at least two months before the SSW onset, contrasting with a decrease in ozone content during the same period in the years before and after SSW. The EH contributed the most to this phenomenon

because the average ozone results of these five stations were similar to those of all ten stations. That is, there was an increase in ozone column during the two months before an SSW onset and a decrease in ozone column during the same period in the pre-SSW and post-SSW years. The phenomenon is less pronounced in the WH. The calculation of the climatology and percentiles shown in Figure 4 is made over the years 1979–2022, with the zero day being the average of the SSW key dates for 1988, 2002, and 2019. Comparison of the middle and bottom rows of panels in Figure 4 indicates that a minimum in TOC is climatologically reached later in the WH stations compared to the EH stations (by ~10 days or more). A similar but more obviously asymmetric response is seen in the SSW years, with pronounced increases in ozone tending to occur much earlier in the EH stations (by ~1–2 months) compared with the WH stations. Similar hemispheric asymmetry was apparent for the minor warming in 2024 due to the focus of upward and poleward planetary wave activity tending to favor the eastern longitudes of the Antarctic region (Zi et al., 2025a).

The TOC value anomalies averaged over ten stations are shown in Figure 5. The SSW years are characterized by positive high TOC anomalies, typically varying from 100 to 150 DU relative to climatology. However, TOC anomalies depend on location. During the SSW of 1988, anomalies over the WH remained comparatively small, in contrast to the EH, where the maximum difference between TOC and climatology exceeded 150 DU. This effect can be due to the displacement of the polar vortex, which covers stations in the WH more often than in the EH. However, the SSWs in 2002 and 2019 do not have such a feature, and ozone anomalies were more uniform in the two hemispheres. A feature of the EH TOC anomaly time series (Figure 5, lower panel) is quasi-periodic oscillations with an approximate period of ~10 days and an amplitude of around 50 DU prior to the SSWs of 1988 and 2002. These oscillations are less coherent in 2019 and likely relate to the interaction of travelling and stationary planetary waves.

In Figure 6, we calculated the TOC for the day of the year corresponding to the center date of the SSW and for 60 days before and after onset (zero) day, for three years before and after the SSW event. Then, for each day, we calculated the difference with the climatology and averaged the data for years before and after the SSW. Finally, we averaged TOC anomalies corresponding to the same time lag for three SSW events in 1988, 2002, and 2019.

For several stations (Amundsen-Scott, Davis, Syowa), a trend indicating a decrease in TOC is apparent before and after the SSW. For the other stations (Rothera, Faraday/Vernadsky), the variations of TOC before and after the SSW are anticorrelated. For the whole set of stations, no clear trend is noticed.

TOC variations at each station facilitate a detailed study of how TOC values vary in the year before, the SSW year, and the year after SSW, to identify similarities and differences in TOC across all regions where the stations are located. We retrieve TOC values for each day within ±60 days relative to the SSW onset for the years 1988, 2002, and 2019, as well as the adjacent years, at each WH and EH station shown in Figures A1.1–A1.3 (Appendix 1).

A review of Figures A1.1, A1.2, and A1.3 provides the insights into the effect of the warming, depending on a station's location. During these SSW events, the highest values of TOC were observed at the sub-Antarctic stations, in Ushuaia in the WH, and at Macquarie Island in the EH, respectively. The lowest values were observed at Amundsen-Scott and Halley in the WH and at Syowa in the EH. However, in the SSW years, extremes at these particular stations did not occur.

The maximum TOC during SSWs in the WH was observed a few days after the day of the event, contrary to the EH, where TOC peaks were observed with a positive time lag. As was mentioned before, in the WH, the increase of TOC during each SSW was near zero. Extremely low values of TOC during the SSW in 2019 were observed at Syowa from ~10 to ~40 days after the event (see Figure A1.3).

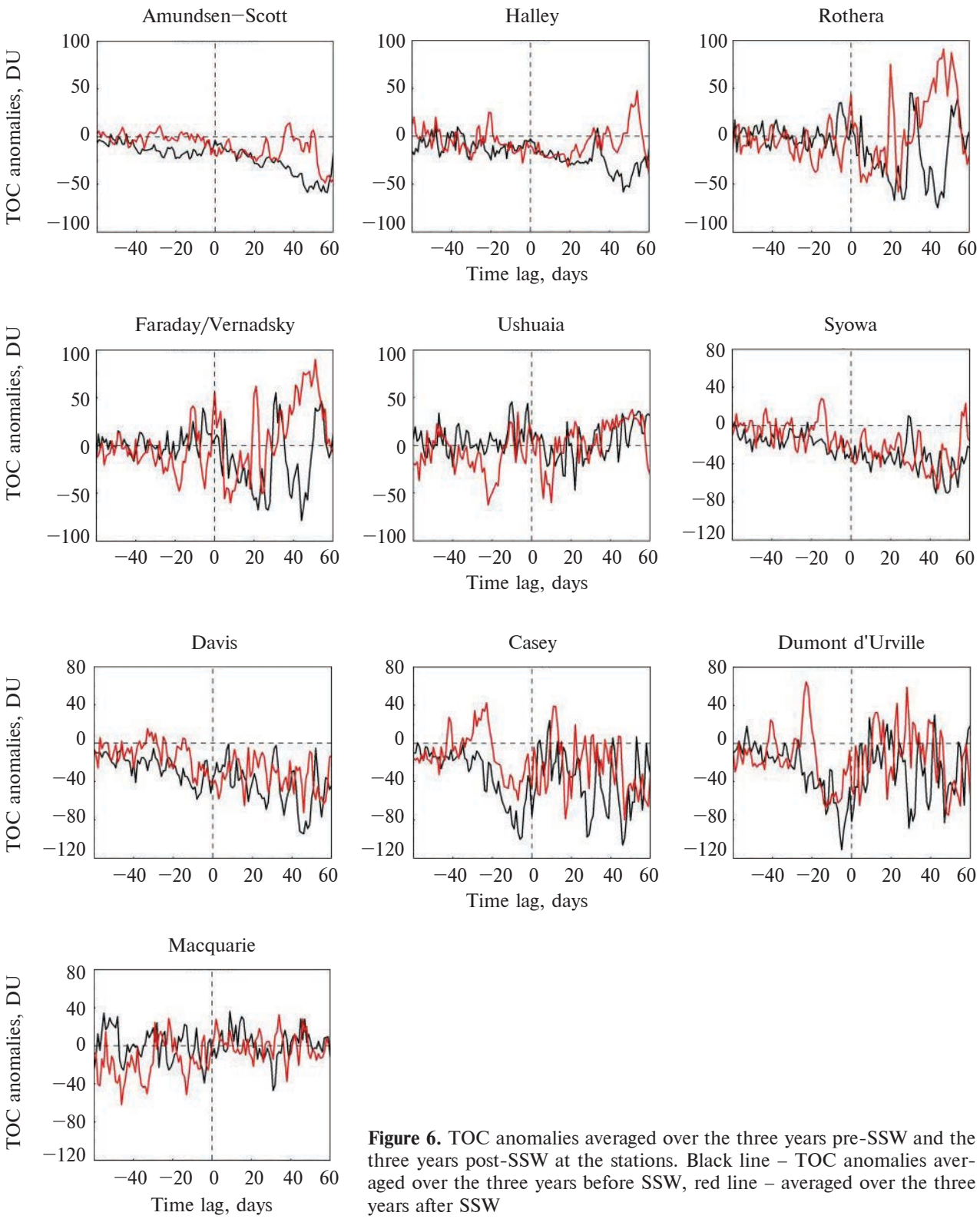


**Figure 6.** TOC anomalies averaged over the three years pre-SSW and the three years post-SSW at the stations. Black line – TOC anomalies averaged over the three years before SSW, red line – averaged over the three years after SSW

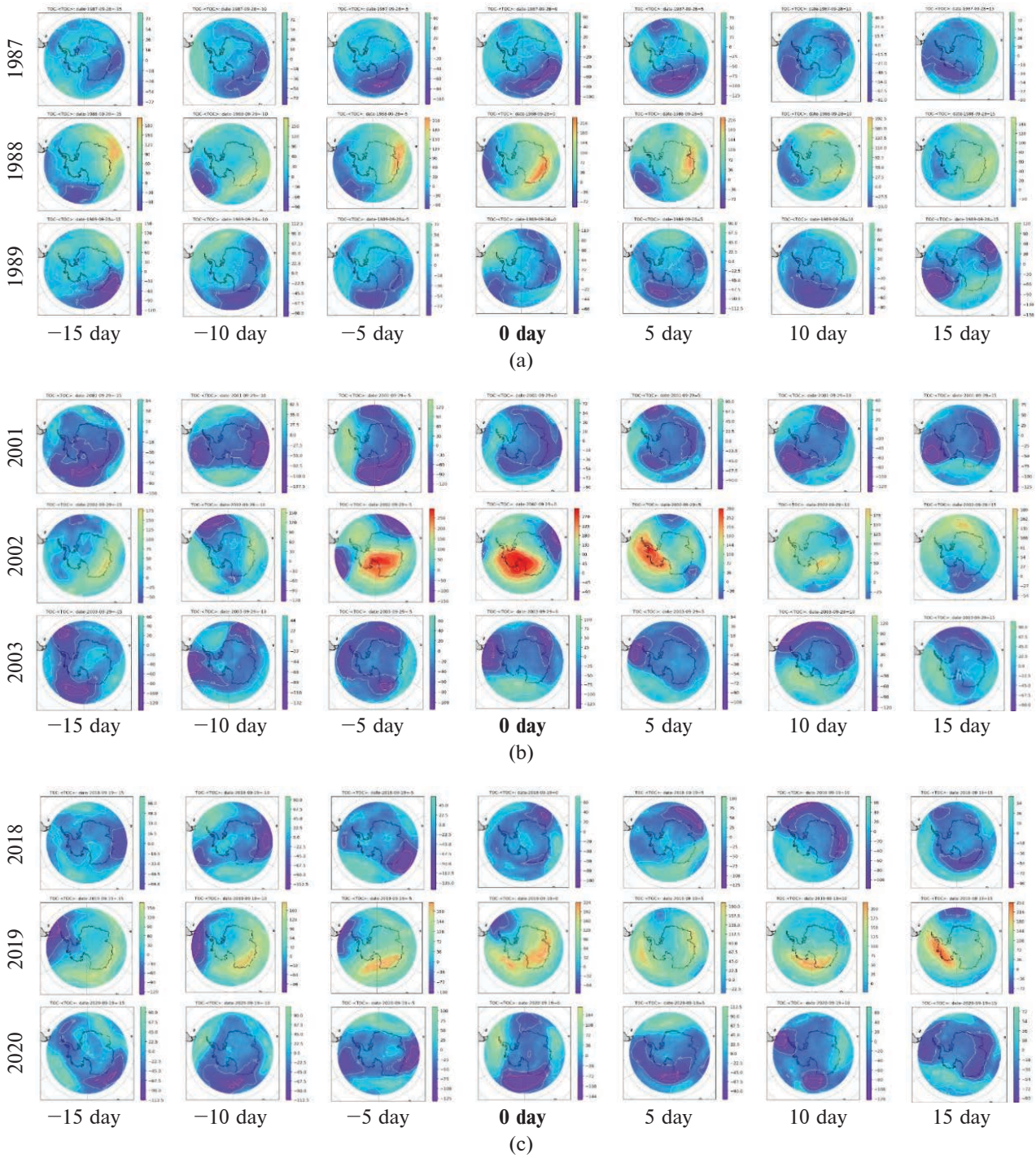


**Figure 7.** Ozone anomaly fields on −15 day to +15 day around 0 day for (a) SSW1988, (b) SSW2002, (c) SSW2019 over Antarctica in the one pre-SSW, SSW, and one post-SSW year. All the TOC anomaly maps are constructed using the same color scale. The scale next to each panel map indicates the TOC anomaly range in DU

### 3.2 TOC anomaly fields by MSR-2 data

Maps of total ozone anomalies around the SSW onset ("0") date are shown in Figure 7. The panels show ozone anomaly fields made using the difference ("anomaly") between the TOC field for 1988, 2002, and 2019 ("0" days are 28 September 1988, 29 September 2002, and 19 September 2019) and the averaged TOC for 1979–2022 (excluding the years 1988, 2002, 2019) for the 15th, 10th, and 5th days before the "0" day and the 15th, 10th, 5th days after it. Note that all the TOC anomaly maps in Figures 7, 8, and Figure A2.1 are created in the general standard color scale dependent on TOC values. The scale next to each panel map indicates the TOC anomaly range in DU at the specific map. Therefore, all maps are comparable by color.

In terms of the main features in Figure 7, firstly, there is a clear distinction between the anomalies in the SSW years and the immediately adjacent years. In all cases, positive anomalies exceeding 100 DU cover large areas over East Antarctica or the adjacent ocean. These anomalies persist around the SSW onset date throughout the entire analyzed monthly range and are also evident in daily fields (see Figure A3.2 in Appendix 3). The ozone anomaly field in 2002 is unique for all years, exceeding the climatological means by 250 DU during ±5 days around the onset date. This feature indicates that the major warming in 2002 had an exceptional influence on the Antarctic ozone distribution.

The ozone anomalies in 1988 and 2019 were smaller (~150 DU), but in 2019, the SSW expanded farther into the inner region of the stratospheric polar vortex than it did in 1988. All the adjacent years are characterized by prevailing negative anomalies. Their spatial location varied, but ozone reduction was frequently observed around the climatological zonal maximum in the Australian longitudinal sector. The adjacent years demonstrated lower ozone values than climatology, which are most noticeable in 2001, 2003, 2018, and 2020. Typical anomalies over the Antarctic interior are in the range of −50 to −100 DU.

Further details in ozone anomaly fields are seen in the averaged by 30 days pre- and post-

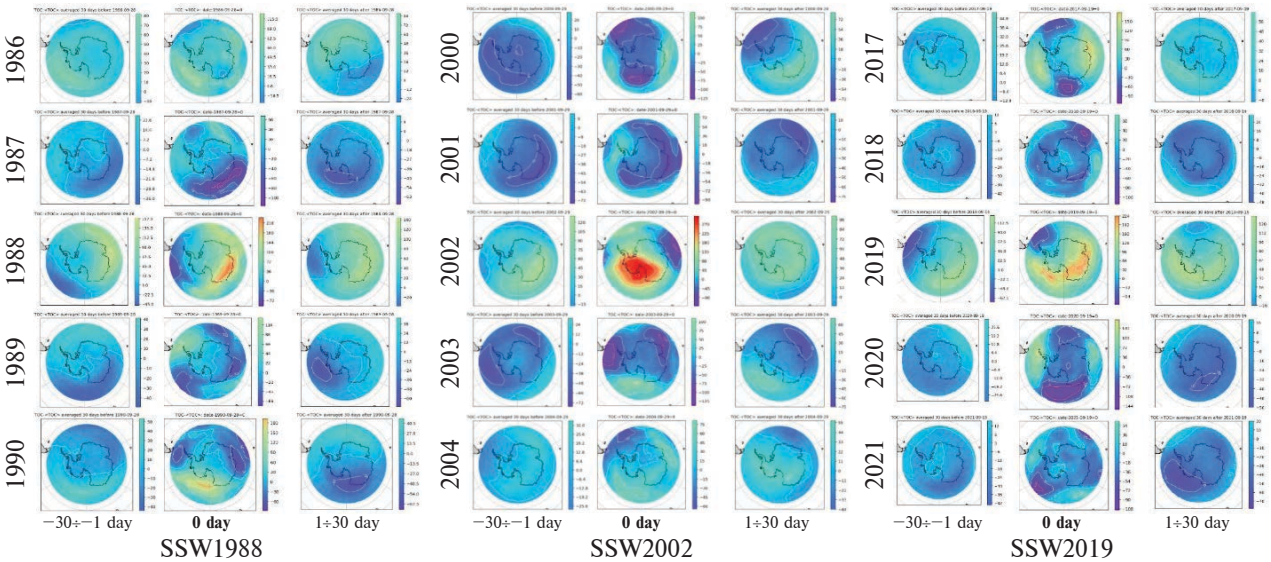


**Figure 8.** Groups of panels left to right: TOC anomalies for SSW1988, SSW2002, and SSW2019, spanning the 2 years before corresponding SSW year and 2 years after corresponding SSW year (rows top to bottom) and for averages of 30 days prior to the SSW 0 date, on the SSW 0 date, and averaged for 30 days after the SSW 0 date (columns left to right for each SSW). The scale in DU is shown to the right of each panel. The colour scale is the same as that used in Figure 7

SSW patterns in Figure 8. Generally, the focus of the strong total ozone enhancement during the SSW occurs in the same geographical region in the month before and after each SSW. For the years immediately preceding and following each SSW, strong contrasts in the monthly averaged data are absent.

## 4 Discussion

While the SSW events of 1988, 2002, and 2019 have been the subject of various studies, still more research is needed to explain their peculiarities and predict conditions of their occurrence. Moreover, further attention is needed more generally on the other stratospheric warmings in the SH, which exhibit less sharp and pronounced changes in stratospheric conditions (Vincent et al., 2022) compared with the three large events.

In comparison to previous analysis (Yu et al., 2025), our study adds to the consideration the spatial distribution of TOC values at selected sites across the Southern Hemisphere. Figures 4 and 5 clearly show that there was a greater amount of ozone in the EH for the SSW years. In the WH, there was no clear difference between SSW and non-SSW years following by 70th-30th percentiles results, and TOC values were very close to the climatology. Quasi-periodic TOC changes associated with travelling planetary waves with a period of about 10 days were observed in 1988 and 2002, but in 2019, there were no obvious variations. It is visible in Figure 5 that quasi-periodic changes in 1988 lasted after the zero date of the SSW. On the contrary, they almost disappeared in 2002. These oscillations are typical for EH stations, being less prominent or practically absent at the WH stations (Fig. 5). Similar oscillations are generally of much smaller amplitude in the years immediately adjacent to the SSW years (see also Yu et al., 2025).

The development of SSW2002 was evidently associated with the exceptional intensity of wave 2 before the 0 date, as clearly shown in Figure A2.1 of Appendix 2. A structure with two maxima is observed prior to the SSW onset date. Following the SSW, the TOC maximum over East Antarctica shifted to the South Pole. Air masses enriched with ozone penetrated to central Antarctica, with the largest influence observed on the days from −4 to +2. In the following days, the ozone-rich region shifted to West Antarctica. Over days 5−9 after zero date, the maximum anomaly was located over the Antarctic Peninsula. After 10 days, the stratospheric vortex over the pole recovered; significant positive anomalies up to 70−90 DU are seen. Interestingly, the EH stations exhibit enhanced TOC values every ~10 days, mainly before the SSWs in 1988 and 2002, but this is not as pronounced in 2019 (which may show more 5-day variability, see Figure 5, lower panel). These peculiarities may be related to the variations in planetary wave activity at 50 hPa across different years (see Figures A3.1 and A3.2 in Appendix 3).

Significant influences on the generation of planetary waves and their propagation into the polar stratosphere are promoted in tropical latitudes by the QBO and patterns of sea surface temperature contrasts, principally those associated with the ENSO phenomenon. Relationships between the QBO and the polar vortex state have been intensively discussed since the 1980s (Holton & Tan, 1982). For the Northern Hemisphere, stratospheric data have demonstrated that the easterly QBO phase is more typical for major SSWs (Watson & Gray, 2014). For the Southern Hemisphere, a few authors have examined this association.

Newman and Nash (2005) mention that the 2002 SSW was accompanied by the westerly phase of the QBO at 20−30 hPa in July (their Figure 4b), but do not explore this feature in detail. They identify the strengthening of the zonal-mean zonal wind as a preconditioning stage and associate the development of the warming with enhanced planetary wave activity in the tropics. Nordström and Seppälä (2021) consider that the deceleration of the polar vortex in 2002 was influenced by both the stratospheric QBO and the mesospheric semi-annual oscillation (SAO). These authors analyzed early winter data at 10 hPa (QBO) and 1 hPa

(SAO) and found that each of the years 1988, 2002, and 2019 demonstrated an easterly QBO phase in the mean June–July 10-hPa winds. Nordström and Seppälä (2021) concluded that the particular prevailing phases of both the QBO and SAO carried enhanced easterly momentum, which significantly weakened the stratospheric polar vortex. The connection between the QBO easterly phase and early spring warming in 2019 was also noted in Eswaraiah et al. (2020).

On average, at all stations in 2002 and 2019, the TOC values are much lower than the TOC climatology. We observe a tendency towards underestimation that is possibly impacted by QBO. By data from (https://acd-ext.gsfc.nasa.gov/Data_services/met/qbo/), we obtain that in September, at the level of 10 hPa in the stratosphere, according to the Singapore sonde zonal wind speed data, a significant easterly wind was observed in the warming years: in 1988 of −34.0 m $s^{-1}$, in 2002 of −22.2 m $s^{-1}$, and in 2019 an easterly zonal wind of −32.0 m $s^{-1}$, but in the pre-SSW and post-SSW years, a predominantly westerly wind was recorded (except for the 2020 event when the easterly wind of −11.1 m $s^{-1}$ was observed). At the same time, the strongest SSW event in 2002 occurs on a significant but the weakest of these three cases of easterly wind. Therefore, the influence of the QBO can be considered as only one of the factors accompanying the appearance of the SSW.

It should be noted that the strongest easterly wind in September, according to the Singapore sonde data, was observed in 1986 (−38.3 m $s^{-1}$). This year, a small ozone hole was observed, but it is not considered to be particularly extreme in Antarctica. Although this confirms the observation, which applies to the Northern Hemisphere, that major SSW events tend to occur during strong easterly QBO conditions, when the stratospheric movement at low latitudes opposes the direction of flow within the polar vortex. Corresponding processes, by all indications, also occur in the polar regions of the Southern Hemisphere.

In terms of the planetary wave influences of ENSO, according to Zi et al. (2025b), higher temperatures in the Niño4 region of the central Pacific Ocean led to stronger planetary wave activity and more significant meridional circulation, with the following weakening of the stratospheric

**Table.** ENSO, QBO, and Coupled mode (CM) indices in pre-SSW, SSW (bold font), and post-SSW years

| Year | ENSO Index[1] | ENSO Type[1] | QBO Index[2] | QBO Type[2] | CM Index[3] | CM Type |
|---|---|---|---|---|---|---|
| 1987 | 1.7 | E | 10.5 | W | −1.8 | STRONG |
| **1988** | **−1.2** | **L** | **2.3** | **W** | **1.5** | **WEAK** |
| 1989 | −0.3 | N | −14.2 | E | −0.8 | NEUTRAL STRONG |
| 2001 | −0.2 | N | −9.7 | E | −1.4 | STRONG |
| **2002** | **0.9** | **E** | **13.5** | **W** | **2.5** | **WEAK** |
| 2003 | 0.3 | N | −17.9 | E | 0.4 | NEUTRAL WEAK |
| 2018 | 0.4 | N | −5.3 | E | −1 | STRONG |
| **2019** | **0.2** | **N** | **12.9** | **W** | **2.5** | **WEAK** |
| 2020 | −0.5 | L | 12.6 | W | −1.6 | STRONG |

*Note:* [1] ENSO 3.4 September index from HadISST1 (https://hadleyserver.metoffice.gov.uk/hadisst/). Index values are expressed as anomalies in °C with respect to the 1980–2010 climatology. E = El Niño, L = La Niña, N = neutral pattern. [2] QBO 30 hPa September index (cpc.ncep.noaa.gov/data/indices/qbo.u30.index). Index values are expressed as equatorial zonal wind anomalies in m $s^{-1}$ with respect to the 1980–2010 climatology. E =eastward, W =westward. [3] Coupled Mode index (Lim et al., 2018). Values are expressed as standard deviations evaluated over April–March from ERA5 (Hersbach et al., 2020) monthly zonal wind anomalies with respect to the 1979–2017 climatology at 55–65°S.

polar vortex. The El Niño phase was in effect before the warmings of 1988 and 2019, but the conditions of 2001/2002 were interpreted as neutral. In general, the frequency of SSWs depends on climate changes, and these events may become less frequent in the second half of the 21st century under current tendencies (Jucker et al., 2021).

As follows from Table, a weak vortex was observed in every SSW year based on the Coupled Mode (CM) index, which measures the strength of the winter polar vortex. For the pre-SSW years, in all cases, the CM index was strong. For the post-SSW years, the CM index was more neutral in 1989 (neutral-strong) and 2003 (neutral-weak), and strong in 2020. In all SSW years, the QBO type was westward (both during the SSW and 2 months earlier), which is consistent with a weak vortex (see Table). In 2020, ENSO was also in the westward mode, but the CM index indicated a strong vortex, making this as a contrary case. ENSO effects can take 1–2 months to propagate to the Antarctic stratosphere (Niu et al., 2023). The July ENSO phase (not shown in Table) was La Niña in 1988, but El Niño in 2002 and 2019. Otherwise, ENSO was neutral in the years surrounding 2002 and 2019, and also in 1989, but an El Niño occurred in 1987. Overall, the SSW years preferentially show a westward QBO and a weak vortex, and tend to favor ENSO conditions. Also, the immediate years straddling the SSW years tend to show a strong vortex, neutral ENSO conditions, and an eastward QBO.

Considering the unusual TOC values behavior in the period before the SSW onset, the deviations in TOC from the climatology suggest that each warming had been building up over the preceding few months. This behavior is absent in the years immediately surrounding each SSW.

## 5 Conclusions

In this paper, we have studied total ozone variations over Antarctica near the central dates of SSW events in 1988, 2002 (a major warming year), and 2019, in comparison with the respective periods of adjacent years. Multi-Sensor Reanalysis-2 ozone data were analyzed for ten selected Antarctic and sub-Antarctic stations, considering the general ozone distribution in West and East Antarctica. Additionally, the TOC distribution over the entire high-latitude region, southward of 50°S, in the range of 30 days near the warming, was analyzed. The 1979–2022 climatology was used for the comparison.

In comparison with previous studies, our work provides several key enhancements. Specifically, we expanded the analysis to incorporate SSW adjacent years, an aspect that was not explored in previous research. For example, Yu et al. (2025) did not cover deviations from climatology on the maps, limiting anomalies for separate stations. Newman and Nash (2005) analyzed only the years 1988 and 2002, lacking a spatial analysis of preconditions and overlooking adjacent years. Similarly, Shen et al. (2020a; 2020b) discussed three specific SSW events, but their study did not include an analysis of preconditions and adjacent years.

In our analysis, we showed a significant zonal asymmetry in TOC variations across different parts of the Antarctic continent. East Antarctica was characterized by enhanced total ozone before the SSW onset date, and planetary wave-induced variations were strongly focused in this region before (and after) the SSWs. These preconditions were absent in West Antarctica. Total ozone increased over Antarctica near the onset dates of the SSWs, but to a lesser extent in 1988 compared with 2002 and 2019. The stratospheric polar vortex and ozone hole within it are typically located over West Antarctica due to the influence of the quasi-stationary wave with zonal number 1. Therefore, we conclude that dynamical effects during the 1988 SSW did not propagate as strongly to the inner region of the stratospheric polar vortex. This result is supported by the analysis of the TOC spatial distributions. This tendency could be due to a different setup of low-latitude processes in the Antarctic stratosphere in 1988, particularly the prevailing El Niño ENSO phase. In the adjacent years, negative deviations from climatology prevailed.

A key aim of our study is to look for evidence of SSW preconditioning or subsequent follow-on effects. From our TOC maps (Figures 7, 8, and Figure A2.1), a clear difference is evident between the SSW, and both pre-SSW and post-SSW years. In general, the September TOC field in the pre-SSW year is weaker than in SSW year. Further investigation is needed to understand the thermal and dynamical reasons for this preference.

*Author contributions.* Conceptualization, A. G. and G. M.; methodology, A. G., R. Y., A. K., and G. M.; data acquisition, R. Y., A. G., Y. Y., and D. Z.; software, Y. Y., R. Y., A. G., D. Z., and A. K.; validation, A. K., O. E., A. G., and G. M.; investigation and interpretation, R. Y., A. G., A. K., and G. M.; original draft preparation, A. G., A. K., and G. M.; review and editing, A. G., A. K., Y. Y., D. Z., and G. M.; visualization, A. G., R. Y., and D. Z.; supervision, A. G. and G. M.; project administration, G. M. and A. G. Each author contributed to the interpretation and discussion of the results and edited the manuscript. All authors have read and agreed to the published version of the manuscript.

*Acknowledgments.* This work was partially supported by the College of Physics, International Center of Future Science, Jilin University, China, and by the Ministry of Education and Science of Ukraine in the framework of the scientific direction "Mathematical sciences and natural sciences" at Taras Shevchenko National University of Kyiv and project 25BF051-02 (Registration number 0125U002259). This work contributed to the State Institution National Antarctic Scientific Center, Ukraine, research objectives, in particular, project 25DF051-10 (0125U003044). Multi-Sensor Reanalysis TOC values were obtained from the ESA, TEMIS service reanalysis from their website https://temis.nl/protocols/O3global.php. MERRA2 data on planetary wave activity were obtained from https://acd-ext.gsfc.nasa.gov/Data_services/met/metdata/annual/merra2/gph/ provided by the Atmospheric Chemistry and Dynamics Laboratory, NASA Goddard Space Flight Center (https://acd-ext.gsfc.nasa.gov/).

*Funding.* This research has been supported in part by the Jilin University (Grant Number: G2023129024L).

*Conflicts of Interest.* The authors declare no conflict of interest.

**References**

Baldwin, M., Hirooka, T., O'Neill, A., Yoden, S., Charlton, A. J., Hio, Y., Lahoz, W. A., & Mori, A. (2003). Major stratospheric warming in the Southern Hemisphere in 2002: Dynamical aspects of the ozone hole split. *SPARC newsletter*, *20*, 24–26. https://www.atmosp.physics.utoronto.ca/SPARC/News20/20_Baldwin.html

Butler, A. H., & Gerber, E. P. (2018). Optimizing the definition of a sudden stratospheric warming. *Journal of Climate*, *31*(6), 2337–2344. https://doi.org/10.1175/JCLI-D-17-0648.1

Butler, A. H., Seidel, D. J., Hardiman, S. C., Butchart, N., Birner, T., & Match, A. (2015). Defining sudden stratospheric warmings. *Bulletin of the American Meteorological Society, 96*(11), 1913–1928. https://doi.org/10.1175/bams-d-13-00173.1

Butler, A. H., Sjoberg, J. P., Seidel, D. J., & Rosenlof, K. H. (2017). A sudden stratospheric warming compendium. *Earth System Science Data, 9*(1), 63–76. https://doi.org/10.5194/essd-9-63-2017

Charlton, A. J., & Polvani, L. M. (2007). A new look at stratospheric sudden warmings. Part I: climatology and modeling benchmarks. *Journal of Climate*, *20*(3), 449–469. https://doi.org/10.1175/JCLI3996.1

Eswaraiah, S., Kim, J.-H., Lee, W., Hwang, J., Kumar, K. N., & Kim, Y. H. (2020). Unusual changes in the Antarctic middle atmosphere during the 2019 warming in the Southern Hemisphere. *Geophysical Research Letters, 47*(19), e2020GL08919. https://doi.org/10.1029/2020GL089199

Hersbach, H., Bell, B., Berrisford, P., Hirahara, S., Horányi, A., Muñoz-Sabater, J., Nicolas, J., Peubey, C., Radu, R., Schepers, D., Simmons, A., Soci, C., Abdalla, S., Abellan, X., Balsamo, G., Bechtold, P., Biavati, G., Bidlot, J., Bonavita, M., ... & Thépaut, J.-N. (2020). The ERA5 global reanalysis. *Quarterly Journal of the Royal Meteorological Society, 146*(730), 1999–2049. https://doi.org/10.1002/qj.3803

Holton, J. R., & Tan, H.-C. (1982). The quasi-biennial oscillation in the Northern Hemisphere lower stratosphere. *Journal of the Meteorological Society of Japan, Ser. II, 60*(1), 140–148. https://doi.org/10.2151/jmsj1965.60.1_140

Jucker, M., Reichler, T., & Waugh, D. W. (2021). How frequent are Antarctic sudden stratospheric warmings in present and future climate? *Geophysical Re-*

*search Letters*, *48*(11), e2021GL093215. https://doi.org/10.1029/2021GL093215

Kanzawa, H., & Kawaguchi, S. (1990). Large stratospheric sudden warming in Antarctic late winter and shallow ozone hole in 1988. *Geophysical Research Letters*, *17*(1), 77–80. https://doi.org/10.1029/GL017i001p00077

Lim, E.-P., Hendon, H. H., & Thompson, D. W. J. (2018). Seasonal evolution of stratosphere-troposphere coupling in the Southern Hemisphere and implications for the predictability of surface climate. *Journal of Geophysical Research: Atmospheres*, *123*(21), 12002–12016. https://doi.org/10.1029/2018JD029321

Lim, E.-P., Hendon, H. H., Butler, A. H., Thompson, D. W. J., Lawrence, Z. D., Scaife, A. A., Shepherd, T. G., Polichtchouk, I., Nakamura, H., Kobayashi, C., Comer, R., Coy, L., Dowdy, A., Garreaud, R. D., Newman, P. A., & Wang, G. (2021). The 2019 Southern Hemisphere stratospheric polar vortex weakening and its impacts. *Bulletin of the American Meteorological Society, 102*(6), E1150–E1171. https://doi.org/10.1175/BAMS-D-20-0112.1

Ma, C., Yang, P., Tan, X., & Bao, M. (2022). Possible causes of the occurrence of a rare Antarctic sudden stratospheric warming in 2019. *Atmosphere*, *13*(1), 147. https://doi.org/10.3390/atmos13010147

Newman, P. A., & Nash, E. R. (2005). The unusual Southern Hemisphere stratosphere winter of 2002. *Journal of the Atmospheric Sciences*, *62*(3), 614–628. https://doi.org/10.1175/JAS-3323.1

Niu, Y., Xie, F., & Wu, S. (2023). ENSO Modoki Impacts on the Interannual Variations of Spring Antarctic Stratospheric Ozone. *Journal of Climate*, *36*(16), 5641–5658. https://doi.org/10.1175/JCLI-D-22-0826.1

Nordström, V. J., & Seppälä, A. (2021). Does the coupling of the semiannual oscillation with the quasi-biennial oscillation provide predictability of Antarctic sudden stratospheric warmings? *Atmospheric Chemistry and Physics*, *21*(17), 12835–12853. https://doi.org/10.5194/acp-21-12835-2021

Schoeberl, M. R. (1988). Dynamics weaken the polar hole. *Nature*, *336*(6198), 420–421. https://doi.org/10.1038/336420a0

Shen, X., Wang, L., & Osprey, S. (2020a). Tropospheric forcing of the 2019 Antarctic sudden stratospheric warming. *Geophysical Research Letters*, *47*(20), e2020GL089343. https://doi.org/10.1029/2020GL089343

Shen, X., Wang, L., & Osprey, S. (2020b). The Southern Hemisphere sudden stratospheric warming of September 2019. *Science Bulletin*, *65*(21), 1800–1802. https://doi.org/10.1016/j.scib.2020.06.028

Vincent, R. A., Kovalam, S., Reid, I. M., Murphy, D. J., & Klekociuk, A. (2022). Southern Hemisphere stratospheric warmings and coupling to the mesosphere-lower thermosphere. *Journal of Geophysical Research: Atmospheres*, *127*(15), e2022JD036558. https://doi.org/10.1029/2022JD036558

Watson, P. A. G., & Gray, L. J. (2014). How does the quasi-biennial oscillation affect the stratospheric polar vortex? *Journal of the Atmospheric Sciences, 71*(1), 391–409. https://doi.org/10.1175/JAS-D-13-096.1

WMO: Commission for Atmospheric Sciences. (1978). *Abridged Final Report of the Seventh Session Manila, 27 February – 10 March (WMO-No. 509)*. WMO. Retrieved August 22, 2025, from https://library.wmo.int/idurl/4/35601

Yu, R., Grytsai, A., Milinevsky, G., Evtushevsky, O., Klekociuk, A., Shi, Y., Poluden, O., Wang, X., & Ivaniha, O. (2025). Zonal asymmetry in ozone variations over Antarctic stations during the life cycle of sudden stratospheric warmings. *Journal of Geophysical Research: Atmospheres*, *130*(12), e2024JD042896. https://doi.org/10.1029/ 2024JD042896

Zi, Y., Long, Z., Sheng, J., Lu, G., Perrie, W., & Xiao, Z. (2025a). The sudden stratospheric warming events in the Antarctic in 2024. *Geophysical Research Letters*, *52*(7), e2025GL115257. https://doi.org/10.1029/2025GL115257

Zi, Y., Long, Z., Sheng, J., Lu, G., Perrie, W., & Xiao, Z. (2025b). Cross–seasonal impact of SST anomalies over the tropical central Pacific Ocean on the Antarctic stratosphere. *EGUsphere, preprint*. https://doi.org/10.5194/egusphere-2025-2990

Received: 17 September 2025
Accepted: 2 December 2025

**Поведінка загального вмісту озону в Антарктиці в роки до раптового стратосферного потепління (РСП), під час РСП та після РСП**

**Жуйсянь Юй[1], Асен Грицай[2, 3], Геннадій Міліневський[1, 2, 4, *], Олександр Євтушевський[3], Юлія Юхимчук[1, 4, **], Діана Зазубик[3], Андрій Клекочук[5]**

[1] Коледж фізики, Міжнародний центр наук майбутнього, Цзілінський університет, м. Чанчунь, 130012, Китай
[2] Державна установа Національний антарктичний науковий центр МОН України, м. Київ, 01601, Україна
[3] Київський національний університет імені Тараса Шевченка, м. Київ, 01601, Україна
[4] Головна астрономічна обсерваторія Національної академії наук України, м. Київ, 03143, Україна
[5] Школа фізики, хімії та наук про Землю, Університет Аделаїди, м. Аделаїда, СА 5005, Австралія

**Автори для кореспонденції:** * milinevskyi@jlu.edu.cn, genmilinevsky@gmail.com; ** yukhymchuk@jlu.edu.cn

**Реферат.** Раптові стратосферні потепління (РСП) – це драматичні події, що характеризуються раптовими та різкими змінами розподілу температури полярної стратосфери, зонального вітру, загального вмісту озону та інших атмосферних параметрів. РСП є звичайним явищем у зимовий сезон у Північній півкулі, але вони рідкісні в стратосфері Антарктики. За весь час спостережень у південній полярній стратосфері спостерігалося лише одне велике РСП (вересень 2002 року). У статті ця подія розглядається разом із попередніми подіями 1988 та 2019 років, які не відповідають визначенню великого РСП, але супроводжувалися значним підвищенням температури та загального вмісту озону, а також уповільненням зонального вітру. Зміни розподілу загального вмісту озону над Антарктикою аналізуються за допомогою даних мультисенсорного реаналізу (MSR-2). Ми побудували й дослідили просторовий розподіл аномалій ЗВО у роки РСП та сусідні з ними. Відзначається значна зональна асиметрія між Західною та Східною півкулями над Антарктидою. У східній антарктичній стратосфері загальний вміст озону збільшується за кілька тижнів до центральної дати потепління, що вказує на передумови для цієї події. Квазіперіодичні коливання, пов'язані з планетарними хвилями, спостерігалися над Східною Антарктидою у 1988 та 2002 роках. Навпаки, загальний вміст озону над Західною Антарктидою не мав чітких ознак до потепління. Потепління мають чітке просторове охоплення: зокрема, подія 1988 року не проникла у внутрішню область стратосферного полярного вихору. У сусідні роки загальний вміст озону був переважно меншим за кліматологічні значення, і ми дійшли висновку, що зниження вмісту озону є найбільш типовим для попередніх років (1987, 2001, 2018).

**Ключові слова:** MSR-2, антарктичні наукові станції, життєвий цикл, загальний вміст озону, планетарні хвилі, раптове стратосферне потепління

**APPENDIX 1. TOC values at each station within ±60 days relative to the SSW onset date**

In Figure A1.1, the upper panel presents plots of TOC values for each day within ±60 days relative to the SSW onset for 1988, and the preceding and following year, at each WH station. The average ozone values for the five WH stations and all ten stations are also provided. The bottom panel is similar to the upper panel, but for five EH stations. Figures A1.2 and A1.3 show the same type of panels for the SSWs in 2002 and 2019, respectively.

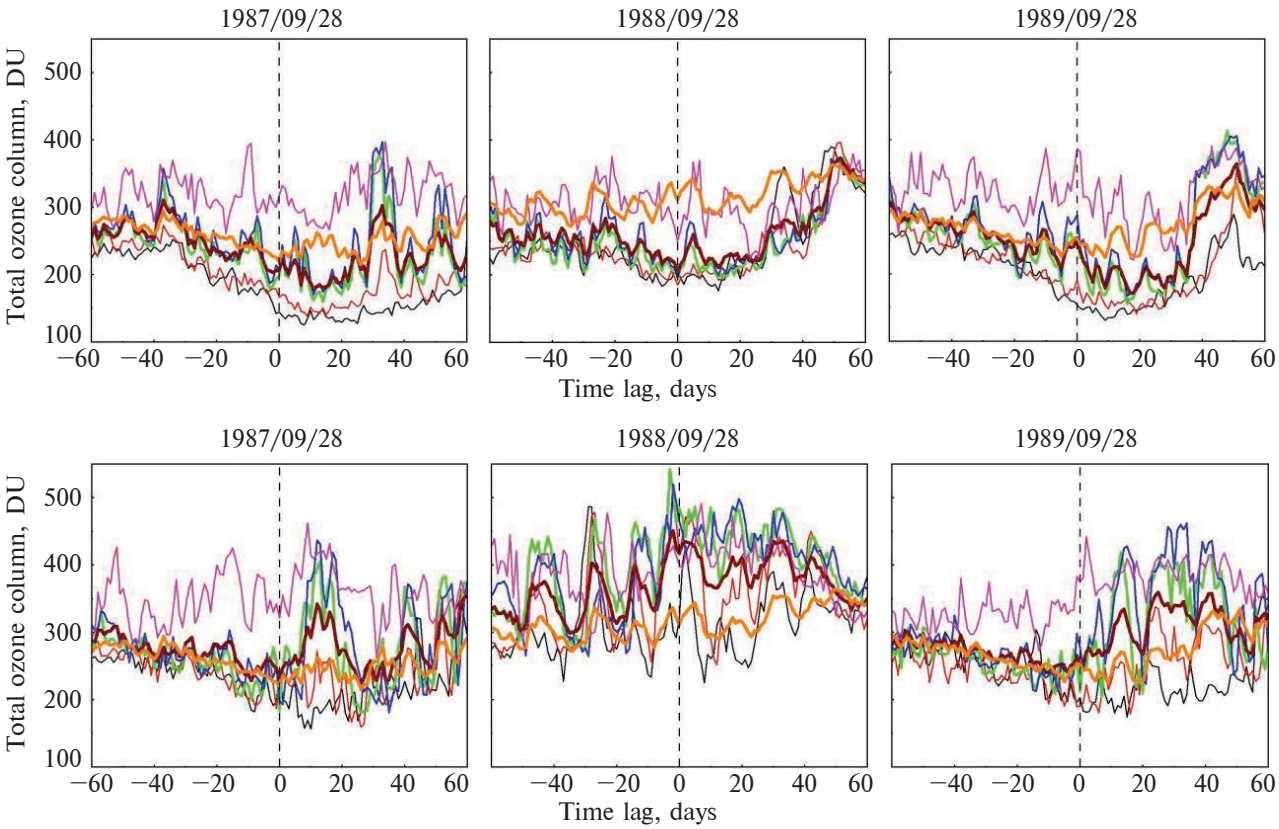


**Figure A1.1.** TOC values for each day within ±60 days relative to the SSW onset date for 1987, 1988 and 1989, at each WH and EH stations. Upper row – WH stations: black line – Amundsen-Scott, orange line – Halley, green line – Rothera, blue line – Faraday/Vernadsky, pink line – Ushuaia, bold brown line – average over 5 WH stations, bold orange line – average over all 10 stations; bottom row – EH stations: black line – Syowa, orange line – Davis, green line – Casey, blue line – Dumont d'Urville, pink line – Macquarie, bold brown line – average over 5 EH stations, bold orange line – average over all 10 stations

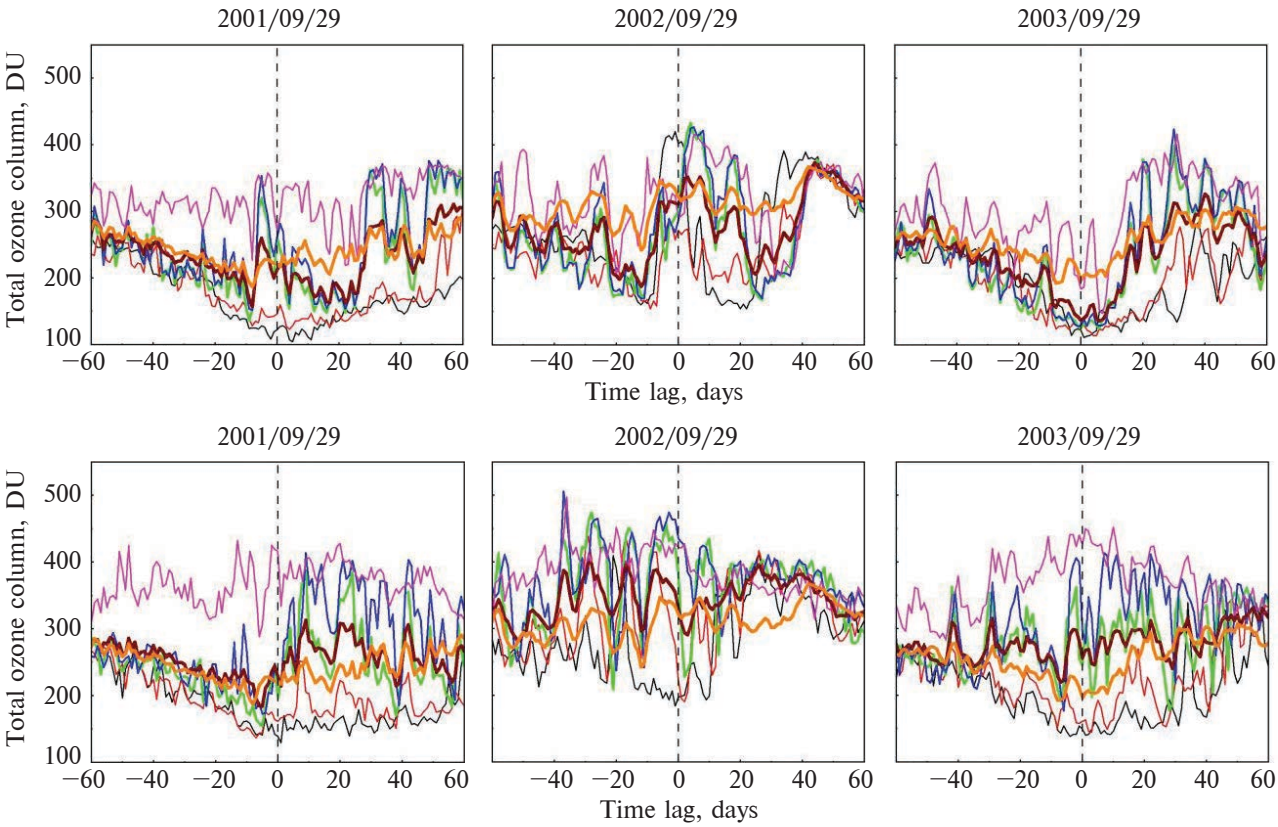


**Figure A1.2.** TOC values for each day within ±60 days relative to the 2002SSW onset date for 2001, 2002, and 2003, at each WH and EH station. Line colors – the same as in Figure A1.1

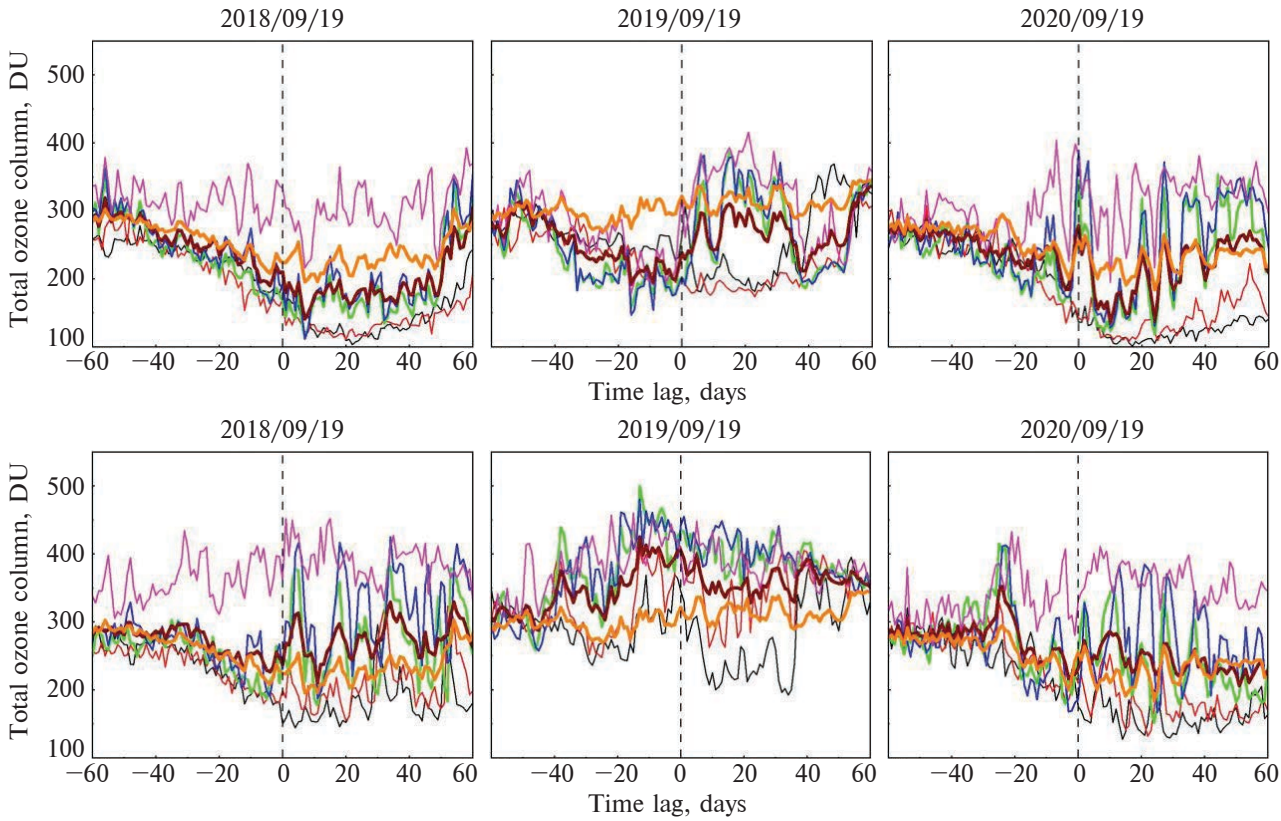


**Figure A1.3.** TOC values for each day within ±60 days relative to the SSW onset date for 2018, 2019, and 2020, at each WH and EH station. Line colors – the same as in Figure A1.1

## APPENDIX 2. TOC daily anomaly fields over Antarctica for the three SSW events

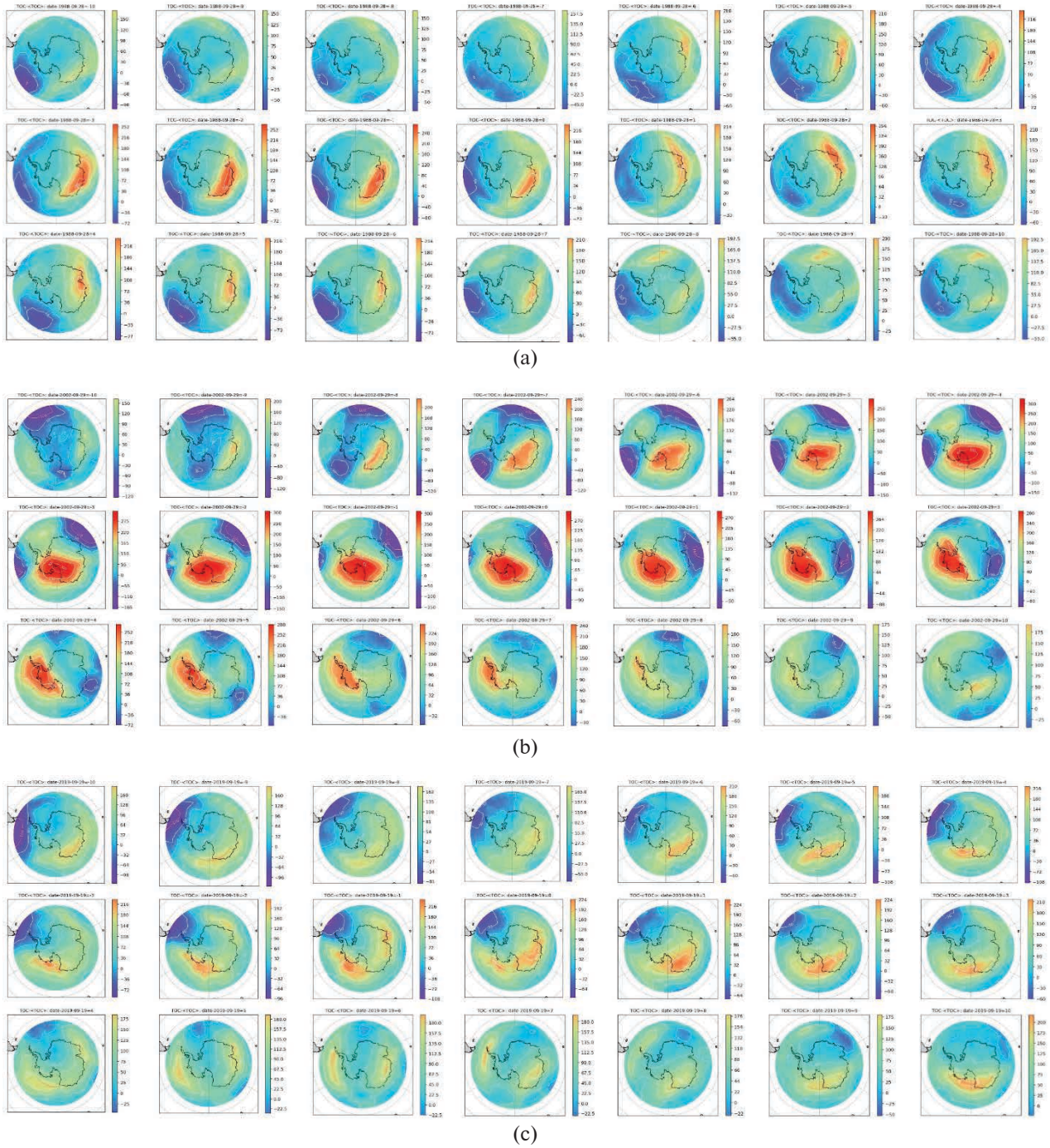

**Figure A2.1.** Ozone daily anomaly fields over Antarctica for (a) SSW1988, (b) SSW2002, and (c) SSW2019 over Antarctica in SSW years. The panels span 10 days before the SSW zero date, the SSW zero date, and to 10 days after the SSW zero date. The scale in DU is shown to the right of each panel. These scales show the range of TOC values in DU, which are present on a specific map

## APPENDIX 3. Planetary wave activity in pre-SSW, SSW and post-SSW years from MERRA2 data

Planetary wave 1 and wave 2 activity at 50 hPa for the pre-SSW, SSW, and post-SSW years are given below in Figures A3.1 and A3.2. Data were obtained from https://acd-ext.gsfc.nasa.gov/Data_services/met/metdata/annual/merra2/gph/ provided by the Atmospheric Chemistry and Dynamics Laboratory, NASA Goddard Space Flight Center (https://acd-ext.gsfc.nasa.gov/).

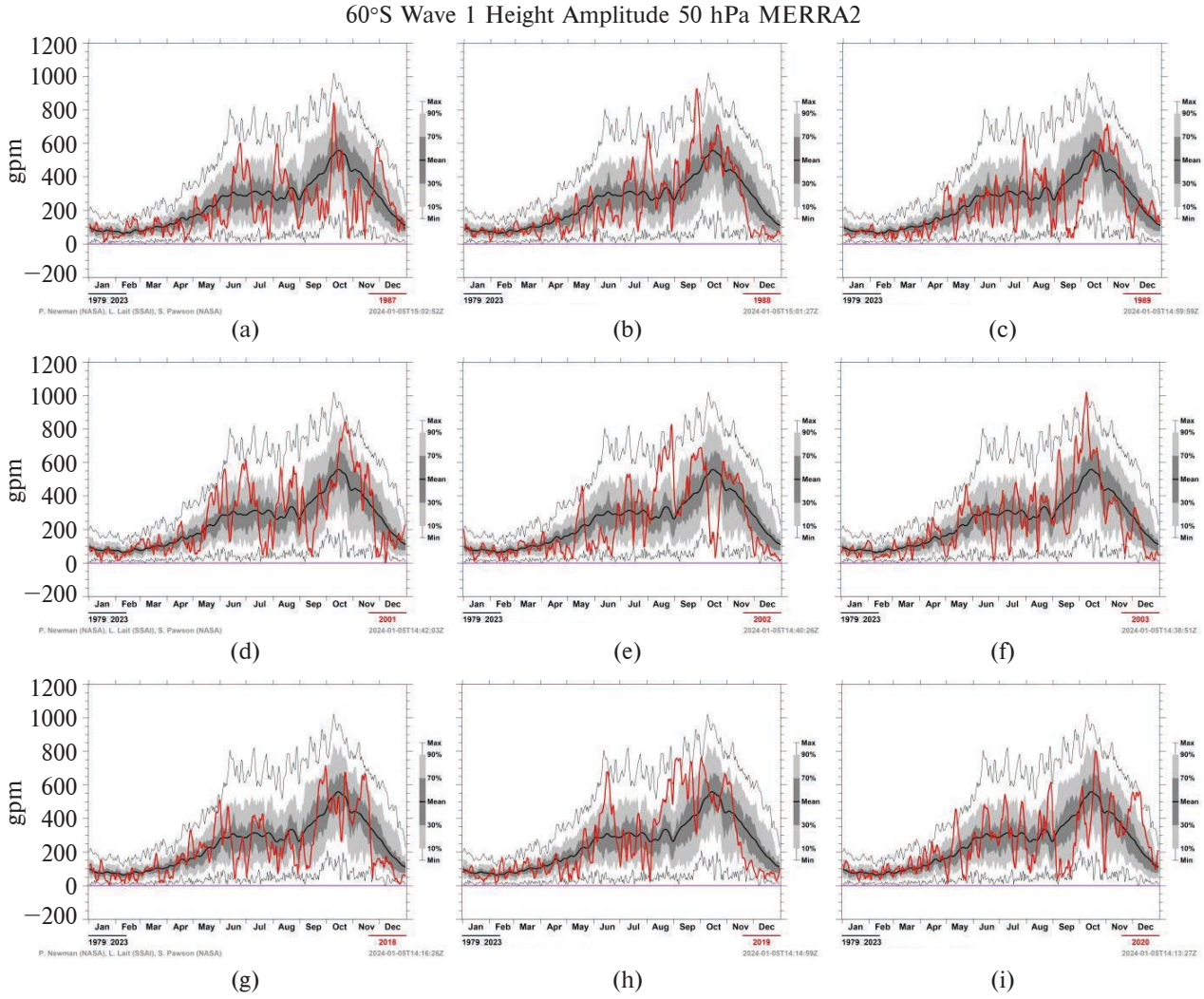


**Figure A3.1.** Planetary wave 1 amplitude at 50 hPa for the pre-SSW, SSW, and post-SSW years, MERRA-2 data

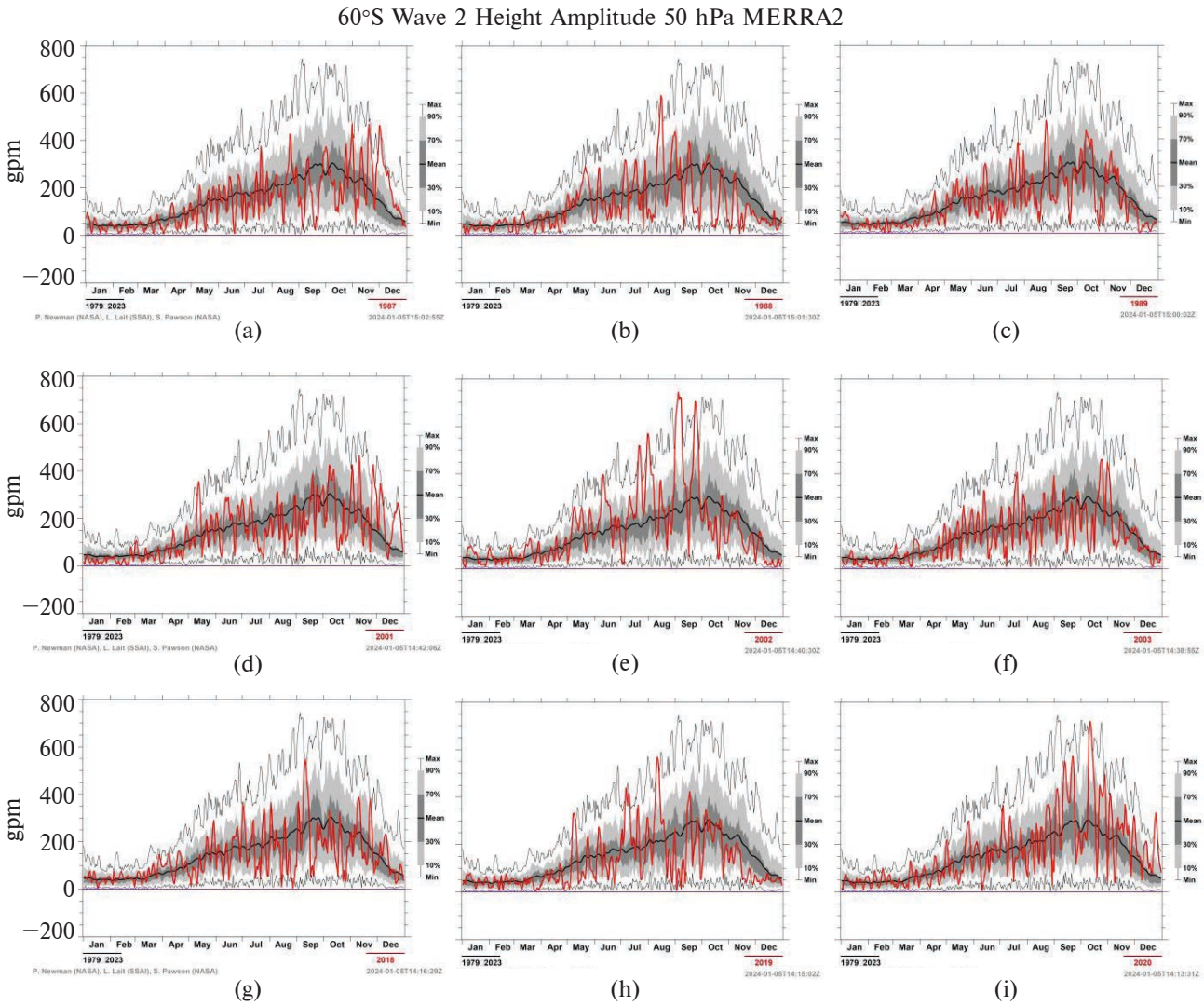


**Figure A3.2.** Planetary wave 2 amplitude at 50 hPa for the pre-SSW, SSW, and post-SSW years, MERRA-2 data